International Journal of Automotive Technology, Vol. 8, No. 6, pp. 799–806 (2007)

1229–9138/2007/037–15

DESIGN OF A SINGLE MODE VARIABLE BRIDGE TYPE SPLIT-POWERED CVT WITH AN INNER-SPHERICAL CONTINUOUSLY VARIABLE UNIT

S. H. SEONG, H. W. LEE*, J. H. CHOI and N. G. PARK

Department of Mechanical Design Engineering, Pusan National University, Busan 609-735, Korea

(Received 23 March 2007; Revised 1 September 2007)

ABSTRACT–One method for improving the torque capacity of the CVT is to use a split-powered CVT (SPCVT) to reduce the power transmitted into a continuously variable unit (CVU). A variable bridge SPCVT with two planetary gear units (PGUs), which are composed of a sun gear, a ring gear, and carrier and planetary gears, can minimize the power to the CVU. However, a SPCVT with a conventional CVT should possess a dual mode, which would allow the conventional CVT to be used at high speeds and an additional gear train to be used at low speeds. The inner-spherical CVU (ISCVU) with an inner and outer spherical contact mechanism developed in this study can cover the range from low to high speeds. The rated power and the overall speed ratios were 100 kW and 0.09~0.36, respectively. Power efficiency was numerically calculated to be over 90% over the speed ratio range of 0.1~0.29. The maximum shear stress at the two contact areas of the rotor pairs, the minimum life and the overall size were estimated to be 700 MPa, 276 kh and 350×350×400 mm^3, respectively. This study shows that an ISCVU and a variable bridge type PGU can realize the SPCVT with a single mode for a vehicle.

KEY WORDS: CVU, CVT, ISCVU, IVT, Overall speed ratio, PGU, Single mode, SPCVT, Variable bridge

1. INTRODUCTION

Recently, there has been growing interest in CVTs, since they are superior to gear trains in terms of controllability and quietness (Tanaka and Eguchi; 1991, Tanaka and Machida, 1996; Shoji and Kawashima, 2003; Carter and Miller, 2003; Pfiffner *et al.*, 2003; Lee and Kim, 2003). However, many recent studies have focused on split-powered CVTs (SPCVTs) in order to reduce the power transmitted into continuously variable units (CVUs) because of the low torque capacity of CVTs (Mucino *et al.*, 2001; Ryu *et al.*, 2002, Russner and Singh, 2004). When using a SPCVT, the coverage of the speed ratio of the CVU should be wider than that of the overall speed ratio. Since the push-belt and toroidal CVUs provide no more than 4.0 of the coverage rate of the speed ratio, their coverage is not wide enough to cover the full range of the overall speed ratio. The push-belt and toroidal CVUs are dual mode models, which are composed of a gear train used at low speed and a CVU used at high speed. Since it is difficult to realize a single mode SPCVT, many studies have recently focused on dual mode CVTs including SPCVTs (Mattson; 1994, Pitchard and Besson, 1981, Walker; 1994). However, such a model, causes the drive train to increase in size, weight and complexity because of the additional dog clutches and synchronizers required.

In this paper, an SPCVT with an ISCVU is conceptually designed. The ISCVU has a high torque capacity since the inner and outer spherical contact mechanisms are geometrically suitable for increasing the torque capacity. Since the shape of the contact area is always circular, there is very little spin loss. The coverage rate of the overall speed ratio of the ISCVT is also infinite (Seong *et al.*, 2005). Among the three SPCVT types (the input-coupled shunt, the output coupled shunt and the variable bridge), the variable bridge most effectively minimizes the power transmitted into the CVU. In addition, the variable bridge type requires an infinitely variable unit on the CVU. The proposed SPCVT consists of a variable bridge type split-power device and an ISCVU. The engine shaft connects with the sun gear in PGU_1 (see Figure 1 (a)). The ring gear in PGU_1 connects directly to the sun gear in PGU_2. The carrier in PGU_1 connects to the carrier in PGU_2. The ring gear in PGU_2 connects to the propeller shaft of the car. Between the ring gear in PGU_1 and the carrier in PGU_2, the ISCVU is connected to the input and output rotors, respectively. This SPCVT operates with a single speed ratio mode. To reverse the vehicle, a one

*Corresponding author. e-mail: rotor@dreamwiz.com

way clutch is installed at the sun gear in PGU_2. The overall power efficiency, contact stresses, and durability of the model are numerically investigated to show the validity of the proposed SPCVT, which combines the variable bridge and the ISCVU with a single mode. To investigate its practicability, the SPCVT is conceptually designed for an automobile with 100kW of power and the overall size of the transmission is estimated. Transmission efficiency is calculated by considering friction loss of the contact area.

2. DESIGN OF THE SPLIT-POWER DEVICE

SPCVTs have been categorized as input-coupled shunt, output-coupled shunt, and variable bridge types. The input coupled shunt uses one set of PGUs. Two of the three central gears in the PGU are connected with the engine shaft and the propeller shaft, respectively. The CVU is inserted between the input gear and the remainder of the central gear. For the output coupled shunt, the CVU is inserted between the output gear and the remainder of the central gear. The power ratio is defined as the ratio between the power transmitted to the CVU and the total power, which is a function of the overall speed ratio. The input- and output-coupled shunt types do not have the maximum or minimum values of the power ratio. Figure 1(a) shows a schematic of the variable bridge type SPCVT. The sun gear 'S_1' in PGU_1 is connected to the engine. The ring gear 'R_1' in PGU_1 connects directly to the sun gear 'S_2' in PGU_2. The carrier 'C_1' in PGU_1 connects with the carrier 'C_2' in PGU_2. The ring gear 'R_2' in PGU_2 connects with the propeller shaft of the car. Between the ring gear 'S_2' in PGU_1 and the carrier 'C_2' of the same PGU, the ISCVU is connected to both gears 'g' and 'a', respectively. As shown in Figure 1(b), the power ratio to the overall speed ratio is as follows:

$$\Psi=\frac{(\delta-B)(\delta-A)}{(B-A)\delta}(A>B), \tag{1}$$

$$A=\frac{R_{S_1}}{R_{C_1}}\frac{R_{C_2}}{R_{R_2}},\ B=\frac{R_{S_1}}{R_{R_1}}\frac{R_{S_2}}{R_{R_2}}, \tag{2), (3}$$

where Ψ is the power ratio, δ is the overall speed ratio, (which is the speed ratio of the SPCVT), A and B are system parameters for the front and PGU_2, and R_{S1}, R_{C1}, R_{R1} are the radii of the sun gear, carrier, and ring gear in PGU_1, and R_{S2}, R_{C2}, R_{R2} are the radii of the same gears in PGU_2.

Equation (1) has an extreme in the middle of the CVU speed ratio defined by:

$$\Psi_0=\frac{\sqrt{A}-\sqrt{B}}{\sqrt{A}+\sqrt{B}}, \tag{4}$$

where Ψ_0 is the maximum power ratio.

According to Chebyshev's approximation, in order to obtain the minimum value, the absolute value of the power ratio at a low speed ratio should be equal to the maximum power ratio, and the power ratio at a high speed ratio should be equal to the maximum power ratio as follows (Cheney, 1966):

$$-\Psi(\delta_1)=\Psi_0 \tag{5}$$

$$-\Psi(\delta_2)=\Psi_0, \tag{6}$$

where δ_1 and δ_2 are the lower and upper limit of the overall speed ratio, respectively.

For the given limits of the overall speed ratio, the system parameters A and B are obtained. Thus from equations (2) and (3), we obtain the ratio of the radius of the carrier with respect to the radius of the sun gear. Similarly, the radius of one of the associated ring gears can be obtained.

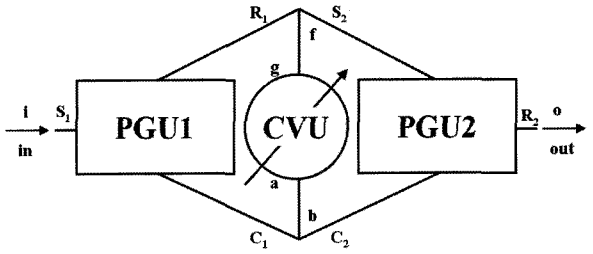

(a) Schematic of the variable bridge type SPCVT

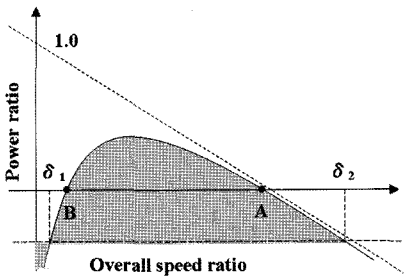

(b) Relationship between the power ratio

Figure 1. Schematic and the power ratio of the variable bridge type SPCVT.

3. DESIGN OF THE ISCVU

The ISCVU shown in Figure 2 consists of three spherical traction rotors, two pressure devices and a set of ratio changer mechanisms. The counter rotor assembly uses the external surfaces of the spheres, and the driving and driven rotors use the internal surfaces of the spheres. The CVU speed ratio is defined as follows:

$$\rho=\frac{h_1}{h_2}\frac{h_3}{h_4}, \tag{7}$$

$$h_1=r_1\sin\theta_1,\ h_2=r_\phi\sin(\theta_1+\phi), \tag{8), (9}$$

$$h_3=r_\phi\sin(\theta_2+\phi),\ h_4=r_2\sin\theta_2, \tag{10), (11}$$

where ρ is the CVU speed ratio and h_1, h_2, h_3 and h_4 are the distances between the rotating axes of the driving (or driven) rotors and the counter rotor ball and the contact points (P_1 and P_2). r_1, r_2 and r_φ are the radii of the driving, driven and counter rotors. φ, θ_1 and θ_2 are the tilting angle and the angles between the rotor axis and the contact point and between the driving and driven rotor, respectively. h_2 and h_3 continuously vary according to the tilting angle. The traction points (P_1, P_2) of both the driving and driven parts are unchanged, while the tilting angle of the rotating axis of the counter rotor varies.

The CVU speed ratio also relates to the overall speed ratio as follows:

$$\rho=\frac{1}{\beta_0}\frac{1-A}{1-B}\frac{\delta-B}{\delta-A}, \tag{12}$$

where β_0 is defined by the product of the gear ratio between the gear 'f' and the input gear 'g' of the CVU and the gear ratio between the connecting gear 'a' and the connecting gear 'b' of the CVU. Thus, the ISCVU when combined with the variable bridge should have zero and infinite speed ratios within the range of the CVU speed ratio. By setting the gear ratio between gear 'R_1' and input gear 'g' to 1.0 and the ratio between output gear 'a' and gear 'C_2' to 0.4826, β_0 becomes 0.4826. In this system, the range of the CVU speed ratio has to be over −0.16 or under −6.38 (Figure 3).

Since the CVU speed ratio contains a zero value and an infinite value of the CVU speed ratio, the ISCVU is referred to as an infinitely variable transmission (IVT). The relationships between the overall speed ratio, the CVU speed ratio and the tilting angle are shown in Figure 3. The lower and upper limits of the tilting angle are −44.53° and +44.5°, respectively. The phase angles of the contact normal lines through the contact points P_1 and P_2 are both 35.3°. Thus, the active spherical surface on the counter rotor is assigned from 0° to 60°. The schematic diagram of the designed counter rotor is shown in Figure 4.

Two outer spherical rotors are directly connected with the shaft. On the shaft, a bearing pedestal is pivoted by two pins on both sides of the horizontal end. The pins are inserted in the frame extending from the case. Thus, the bearing pedestal can be tilted up and down. Tilting is carried out by the cam-follower mechanism. The guiding

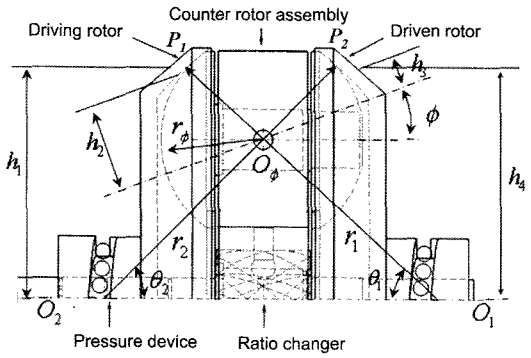

Figure 2. The schematic diagram of the ISCVT.

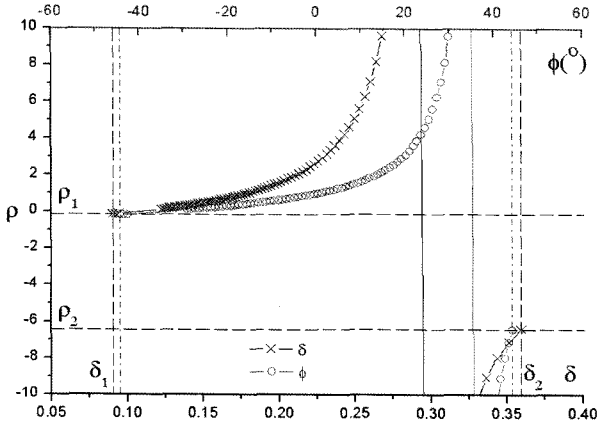

Figure 3. The relationship between δ and ρ with A= 0.2951, B=0.1096 and β_0=−0.4826 (ρ_1=−0.16, ρ_2=−6.38).

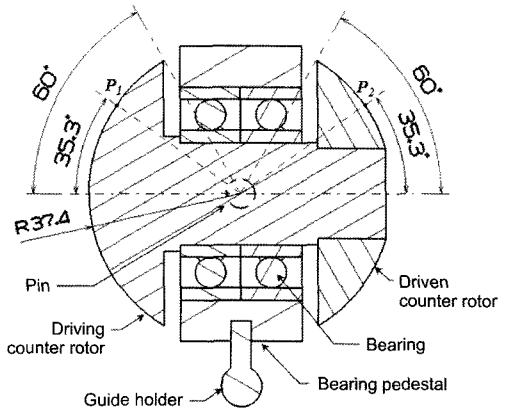

Figure 4. The schematic diagram of the counter rotor assembly.

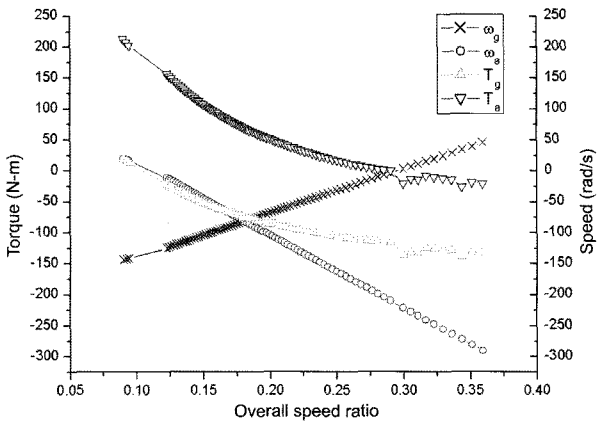

Figure 5. The torque and speed distributions in the input/output shaft of the ISCVU.

groove is set in a core drum, and a ball type guide holder is fixed on the bearing pedestal. By rotating the grooved core drum, the bearing pedestal can also be tilted.

With a given power rating of 100 kW and a rated speed of 500 rad/s, each counter rotor assembly is loaded with 25 kW. Figure 5 shows the torque and speed distributions of the input/output shaft of the ISCVU. The speed of the input rotor of the ISCVU ranges from −143.8 rad/s to 45.5 rad/s and the speed of the output rotor from −290.6 rad/s to 20.0 rad/s.

Figure 5 also shows that the torque acting on the input shaft of the ISCVU is from 19.7 Nm to −132.0 Nm and the torque on the output shaft is from 212.8 Nm to −20.7 Nm. To prevent slippage at the contact areas, two pressure devices are needed at the front and rear rotor pairs of the ISCVU. The optimum thrust force at both sides of the rotor pairs are simulated and shown in Figure 6. The objective function to maximize is the local power efficiency of the ISCVU. The varied thrust forces shown in Figure 6 could be generated by either a proper hydraulic actuator and the controller or a cam-follower type of mechanical actuator (Figure 2).

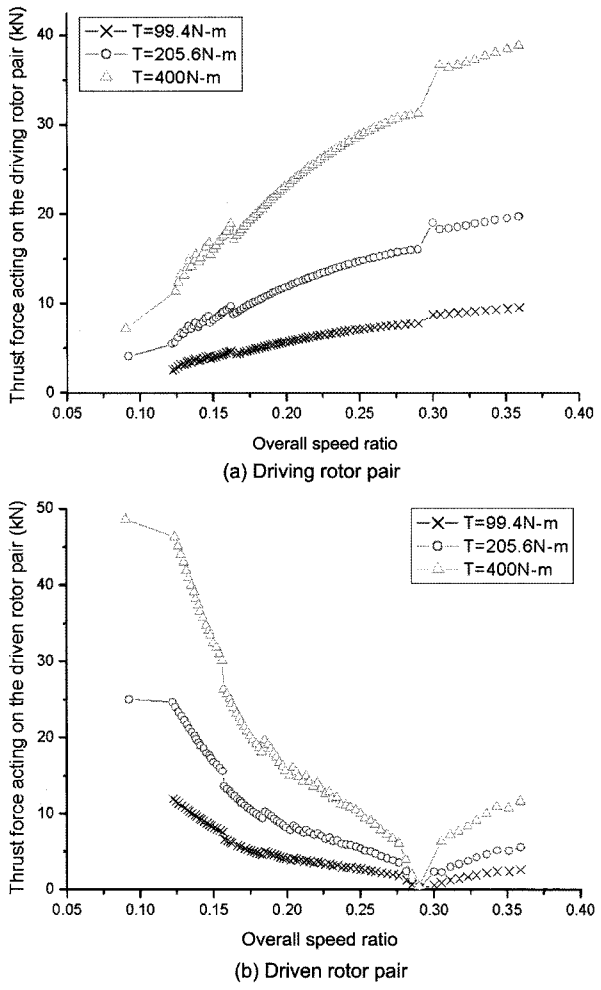

Figure 6. The optimum distribution of the thrust forces to prevent slippage and to minimize spin loss.

4. EFFICIENCY ANALYSIS

The SPCVT is separated into seven parts: gear 'S_1', an assembly of gears (R_1, S_2, f), an assembly of carriers and a gear (C_1, C_2 , b), a planetary gear in PGU_1, a planetary gear in PGU_2, gear 'R_2' and an ISCVU. The governing equations for evaluating the power efficiency of the SPCVT are derived by the kinematic and kinetic relationships of the free body diagrams of the seven parts. The angular velocities and the torques are set to positive values when their directions are counter-clockwise.

For the kinematic relationships of the angular velocities, we have:

$$R_{R1}\omega_{R1}+R_{S1}\omega_{S1}=2R_{C1}\omega_{C1}, \quad (13)$$

$$R_{R2}\omega_{R2}+R_{S2}\omega_{S2}=2R_{C2}\omega_{C2}, \quad (14)$$

$$\omega_{R1}=\omega_{S2},\ \omega_{C1}=\omega_{C2}, \quad (15), (16)$$

$$\omega_a=\rho\eta_\omega^{\alpha}\omega_g,\ \omega_g=\eta_1\omega_{R1}, \text{ and} \quad (17), (18)$$

$$\omega_{C2}=\eta_2\omega_a,\ \omega_{R2}=\delta\omega_{S1}, \quad (19), (20)$$

where R_{R1}, R_{S1}, R_{C1}, R_{R2}, R_{S2} and R_{C2} are the radii of gears R_1, S_1, C_1, R_2, S_2 and C_2, ω_{R1}, ω_{S1}, ω_{C1}, ω_{R2}, ω_{S2}, ω_{C2}, ω_a and ω_g are angular speed of gears R_1, S_1, C_1, R_2, S_2, C_2, 'a' and 'g', and ς_1 and ς_2 are defined as the gear ratios of gear 'f' to gear 'g' and of gear 'a' to gear 'b', respectively. η_ω is velocity efficiency, which is defined as the ratio of the actual speed of the output rotor to the theoretical speed of the output rotor that does not consider the energy loss. α is set to 1 when the power is transmitted from gear 'g' to gear 'a'; otherwise it is −1.

The kinetic relationships are derived from the torque equilibrium and the energy balance. For gear 'S_1', the assembly of gears (R_1, S_2, f), the assembly of carriers and gear (C_1, C_2, b), and gear 'R_2', we have:

$$\omega_{S1}T_{S1}+\omega_iT_i=0,\ T_{R1}+T_{S1}+T_f=0, \quad (21), (22)$$

$$T_{C1}+T_{C2}+T_b=0,\ T_{R2}+T_o=0, \quad (23), (24)$$

where T_{S1}, T_{R1}, T_{C1}, T_{C2}, T_{R2}, T_b and T_c are the torques of gears S_1, R_1, C_1, C_2, R_2, 'b' and 'c'. T_i and T_o are the input and output torque. For the planetary gear in PGU_1 and the planetary gear in PGU_2, we have:

$$T_{S1}'\omega_{S1}+T_{R1}'\omega_{R1}+T_{C1}'\omega_{C1}=0, \quad (25)$$

$$T_{S1}'+T_{R1}'+T_{C1}'=0, \quad (26)$$

$$T_{R2}'\omega_{R2}+T_{C2}'\omega_{C2}+T_{S2}'\omega_{S2}=0, \text{ and} \quad (27)$$

$$T_{R2}'+T_{C2}'+T_{S2}'=0, \quad (28)$$

Considering the energy loss at the gear contacts and the bearing supports, we have the following energy balance

equations:

$$T_{S1}+\eta_g^{\alpha}T_{S1}'=0,\ T_{R1}+\eta_g^{\alpha}T_{R1}'=0, \quad (29),\ (30)$$

$$T_{C1}+\eta_b^{\alpha}T_{C1}'=0,\ T_{R2}+\eta_g^{\alpha}T_{R2}'=0, \quad (31),\ (32)$$

$$T_{C2}+\eta_b^{\alpha}T_{C2}'=0,\ T_{S2}+\eta_g^{\alpha}T_{S2}'=0, \text{ and} \quad (33),\ (34)$$

$$T_f\omega_f+\eta_g^{\alpha}T_g\omega_g=0, \quad (35)$$

where α is set to 1 when power is transmitted from the central gears to the planetary gears; otherwise it is −1. Similarly, α is set to 1 when power is transmitted from gear 'f' to gear 'g'; otherwise it is −1. The efficiencies of the gear pairs (η_g) and bearings (η_b) supporting the planetary gears are assumed to be 0.99.

The ISCVU consists of a driving rotor, a counter rotor assembly and a driven rotor. For wet friction, the traction coefficient is defined to be the ratio of the shear stress to the normal stress at the infinitesimal area of the contact patch. The traction coefficient is known to be a function of the creep rate and normal pressure. The creep rate is defined as the ratio of the sliding velocity to the rolling velocity at the infinitesimal area of the contact patch. In this paper, the commercial traction fluid of the SANTOTERAC-50 is used for the numerical simulations (Figure 7).

The torque equilibrium equations of the ISCVU are as follows:

$$T_g+\vec{n}_{i0}\cdot\int_{A1}((\vec{r}_1+\vec{\rho}_1)\times\vec{\tau}_1)dA_1=0, \quad (36)$$

$$\vec{n}_{i0}\cdot\left\{\int_{A1}((\vec{r}_1-\vec{a}_1+\vec{\rho}_1)\times\vec{\tau}_1)dA_1+\int_{A2}((\vec{r}_2-\vec{a}_2+\vec{\rho}_2)\times\vec{\tau}_2)dA_2\right\}=0 \quad (37)$$

$$T_a+\vec{n}_{i0}\cdot\int_{A2}((\vec{r}_2+\vec{\rho}_2)\times\vec{\tau}_2)dA_2=0, \quad (38)$$

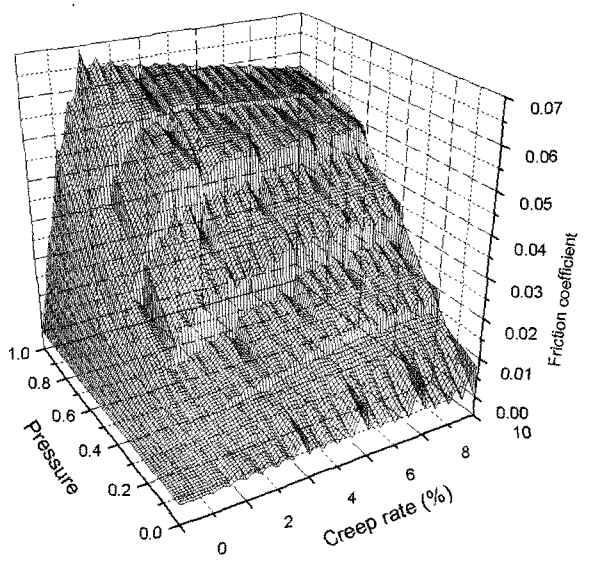

Figure 7. Distribution of the traction coefficient of the SANTOTRAC-50.

where r_1 and r_2 are the radii of the driving and the driven rotor, ρ and n are the local position vector of the infinitesimal area dA and the normal vector in dA, and τ is the shear stress at the contact areas based on Hertz's Contact Theory as follows (Norton, 2000):

$$\vec{\tau}_i=\mu_i p_i\vec{n}_{\vec{\alpha}},\ \mu_i=\mu(Cr_i,p_i), \quad (39),\ (40)$$

$$p_i=p_{i,\max}\sqrt{1-\left(\frac{\rho_{i,r}}{\rho_i}\right)^2},\ p_{i,\max}=\sqrt[3]{\frac{6N_iE_i'}{R_i^2\pi^3}}, \quad (41),\ (42)$$

$$\vec{v}_{ri}=\vec{\omega}_g\times\vec{r}_i,\ \vec{v}_{si}=\vec{\omega}_g\times\vec{r}_i-\vec{\omega}_c\times(\vec{r}_i-\vec{a}_i), \quad (43),\ (44)$$

$$\vec{n}_{\vec{\alpha}}=\frac{\vec{v}_{si}}{|\vec{v}_{si}|},\ Cr_i=\frac{|\vec{v}_{si}|}{|\vec{v}_{ri}|}, \quad (45),\ (46)$$

where i is index 1 or 2 (index 1 is the driving pair of the ISCVU and index 2 is the driven pair), μ is the traction coefficient, p is the normal pressure in the infinitesimal area, v_r is the velocity of the contact point at the input or the output part, v_s is the sliding velocity, and C_r is the creep rate.

Thus, the energy balance equation for the ISCVU is:

$$T_g\omega_g+\eta_c^{\alpha}T_a\omega_a=0, \quad (47)$$

where α is set to 1 when power is transmitted from the gear 'g' to gear 'a'; otherwise it is set to −1. The efficiency of the CVU (η_c) is a function of the velocities and torques of the rotors.

By successive iterative processes, the systems of the kinematic and kinetic equations (13)~(47) are solved. The initial calculation is carried out by assuming no energy loss (that is, η_c=1 and ρ=ρ_0), the first approximate solutions are updated in the successive iterations, and the converse solutions are regarded as the final solutions satisfying the above kinematic and kinetic relationships. Thus, the overall efficiency of the SPCVT is obtained as follows:

$$\eta_t=\frac{\omega_0T_0}{\omega_iT_i}, \quad (48)$$

where η_t is the overall efficiency of the SPCVT.

5. APPLICATION TO THE AUTOMOBILE

To minimize the weight and size of the automobile transmission, the SPCVT model suggested in this paper is conceptually designed for a mid-sized automobile of 100 kW (Figure 8). Engine power passing through the torque converter is transmitted to the sun gear 'S_1' in PGU_1. Power is transmitted by two routes by the planetary gear in PGU_1. Some power is delivered to the rotor assembly connecting the ring gear in PGU_1 to the sun gear in PGU_2. The other power is transmitted through the rotor assembly connecting the carrier in PGU_1 to the carrier in

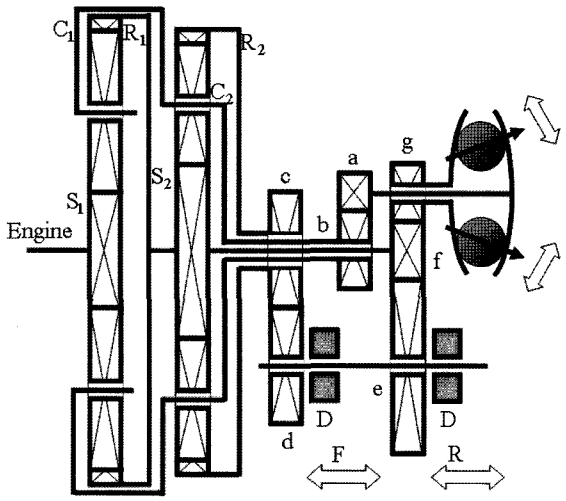

Figure 8. The layout of the SPCVT.

PGU_2. The sun gear in PGU_2 is connected to the input gear 'g' in the ISCVU by the connecting gear 'f'. The output gear 'a' in the ISCVU is connected to the carrier in PGU_2 by the connecting gear 'b'. Finally, the power passing through the sun gear in PGU_2 and the other power which passes through the carrier in PGU_2 are combined and delivered to the ring gear in PGU_2 by the planetary gear of PGU_2. The output power is transmitted to the other shaft by gear stages 'c' and 'd'. This shaft is directly connected to the propeller shaft. The connecting gear 'c' is separated from the shaft. The dog clutch fixes gear 'c' and the shaft to the synchronizer. The reverse mode is carried out by fixing gear 'e' and the secondary shaft with the rear dog clutch and simultaneously releasing gear 'c' and the secondary shaft from the front dog clutch and the synchronizer.

The input speed is rated at 500 rad/s. The overall speed ratio defined as the ratio of the rear wheel speed to the engine speed and ranges from 0.09 to 0.36. With the min-max approximation expressed by equations (5) and (6), parameters A and B are calculated as 0.2951 and 0.1096, respectively. The modules and the number of gear teeth and the widths of the teeth gear element are determined by considering a gear strength equation known as the Lewis Equation with a safety factor of 3. The widths of the teeth are limited 10 to 30 times the width of the pitch. The gears are made from Chromium-Molybdenum alloy steel (AISI4140) with an allowable stress of 218 MPa and a safety factor of 3. The simulation results are listed in Table 1.

The ratio of gears 'f' and 'g' and the ratio of 'a' and 'b' are 1.0 and 0.483, respectively. The design of the SPCVT is based on the final converged solutions for the speed and torque in the nonlinear equations (13)~(48). The overall diameter and width of the ISCVU are within 300 mm and 200 mm, respectively. The overall diameter and width of the variable bridge containing the gear stages are estimated as 310 mm and 300 mm, respectively. Conse-

Table 1. The final results of the gear design (module, number of teeth and face width (mm)).

Split power device	Connecting gear stages
■GU1	■CVU gear stage
- sun gear 'S_1': 2, 24, 36.2	- front gear 'f': 3, 40, 77.7
- planetary gear 'P_1' : 2, 33, 36.2	gear 'g': 3, 40, 77.7 - rear gear 'a': 3, 26, 90.3
- ring gear 'R_1': 2, 90, 36.2	- rear gear 'b': 3, 54, 90.3
■PGU2	■rear gear stage
- sun gear 'S_2': 3, 30, 81.3	- forward gear 'c': 3, 80, 70.0
- planetary gear 'P_2' : 3, 21, 81.3	gear 'd': 3, 80, 70.0 - reverse gear 'e': 3, 120, 77.7
- ring gear 'R_2': 3, 72, 81.3	

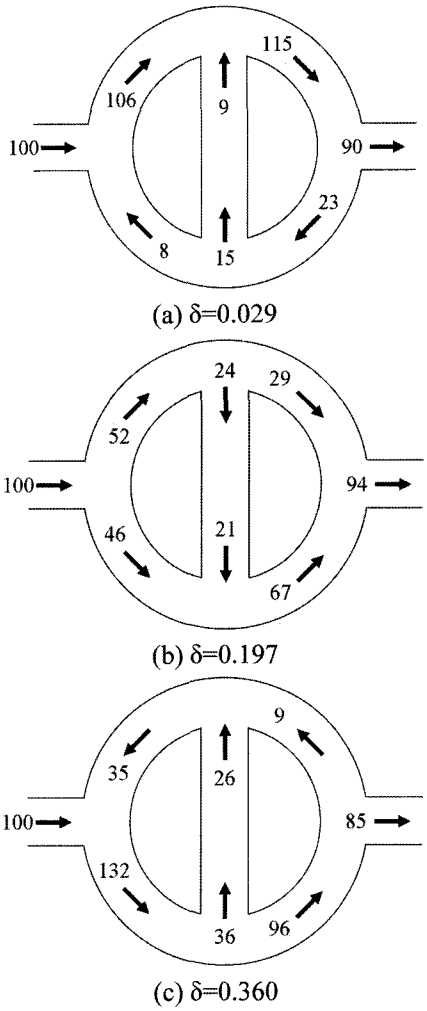

Figure 9. Schematic diagrams for the percent of power flow at 3 speed modes.

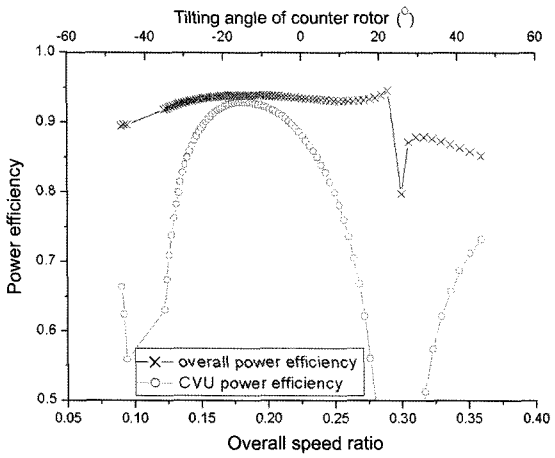

(a) ρ and tilting angles vs power efficiency

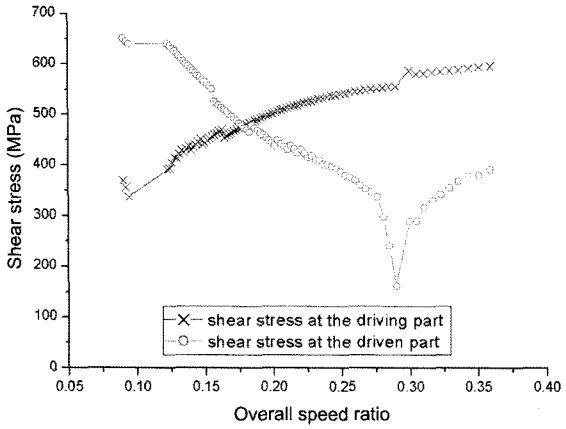

(b) ρ vs shear stress

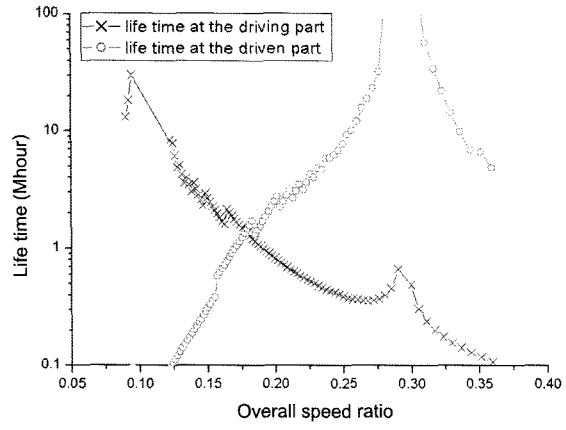

(c) ρ vs life time

Figure 10. Transmission performance of the SPCVT.

quently, the overall size of the SPCVT is estimated to be within 350×350×400 mm^3 from Table 1.

Figure 9 is a diagram of the power flow for the 3 speed modes. At the lowest speed, as shown in Figure 9(a), the

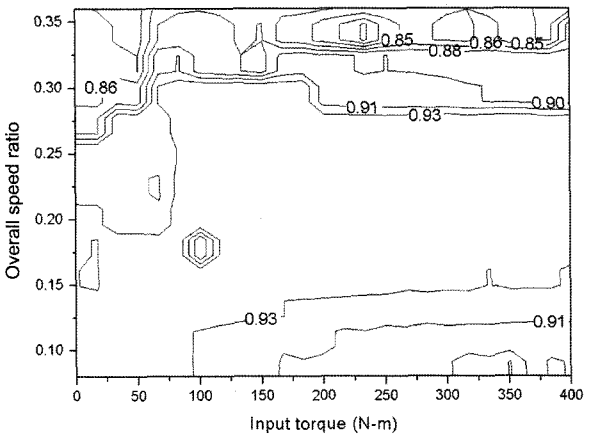

(a) Global efficiencies

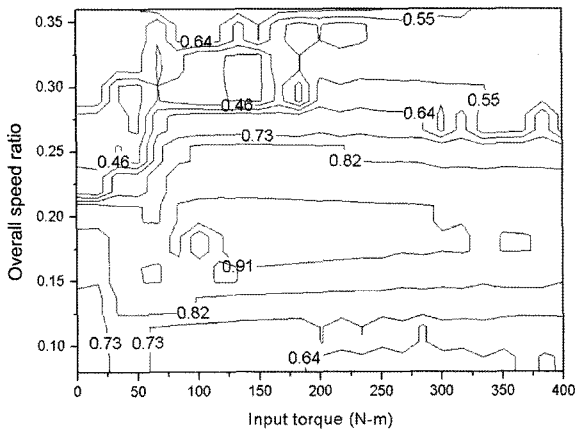

(b) CVU efficiencies

Figure 11. Distribution of the SPCVT efficiencies.

power circulation in PGU_2 runs counter-clockwise, which results in 115% of the power overflowing between the sun gear and the pinion gear in PGU_2. At the highest speed, Figure 9(c), the power circulation in PGU_1 runs counterclockwise as well, which results in 135% of the power flowing between the pinion gear and the carrier in PGU_1.

Figure 10 shows the power efficiencies, the shear stress and the life of the contact area of the CVU. Using the split-power device results in high overall efficiency with values over 90%, even though the efficiency of the CVU is less (Figure 10(a)). The efficiencies in the CVU vary significantly at speed modes approaching Ψ=0. The reason for this is that the ratio of the spin loss with respect to the transmitted power is relatively large in that region. The distribution of the shear stress at the driving and driven parts of rotor pairs is below 700 MPa. Thus, selecting the material for the traction rotors would not be difficult. The life is calculated by the Palmgreen-Lunderberg Equation (Heilch, 1983). The life of each mode is over 100,000 hours and the geometric average values of

the driving and driven rotor pairs are 276,000 and 60,800,000 hours, respectively. The numerical estimations of the transmission performance are shown to have high and slightly varied efficiency along the whole range of speed ratios, small contact stress and long product life.

Figure 11 shows the distribution of the overall and CVU efficiency with respect to speed rated at 500 rad/s. Since the CVU efficiency requires a large coverage rate, there is great variation over the speed ratio range. When the power ratio is 0, efficiency is low since the CVU speed ratio is in the range of zero or infinity. However, overall efficiency is shown to remain higher than 90%. The best distribution of the overall efficiency is in the middle speed range where the overall efficiency is higher than 85% in the range of 2 times the rated torque of 200 N-m as shown in Figure 11(a).

6. CONCLUSION

To operate a single mode transmission, an SPCVT model combining a variable bridge type split-power device with an ISCVU functioning as the IVT is proposed and numerically investigated for the application to vehicles. A variable bridge type PGU transmitting 25% of the input power into the CVU was designed. By controlling the overall speed ratio with a single mode and the tilting angle of the counter rotor ranging from –44.5° to +44.5°, a ratio changer could be properly operated by a camfollower mechanism. For simulating the transmission performances of this model, an SPCVT was conceptually designed with a rated power of 100 kW. The overall size was estimated to be 350×350×400 mm^3. The distribution of the thrust forces acting on the contact areas of the traction drive was simulated with the objective of maximum power efficiency. The thrust force can be easily generated by a pressure device that could be of any type such as a camfollower mechanism, hydraulic actuator or any other configuration.

REFERENCES

Carter, J. and Miller, D. (2003). The design and analysis of an alternative traction drive CVT. *Transmission & Driveline Systems Symp., SAE Paper No.* 2003-01-0970, Detroit, Michigan, USA.

Cheney, E. W. (1966). *Introduction to Approximation Theory.* McGraw-Hill. New York.

Heilch III, F. W. and Shube, E. E. (1983). *Traction Drives; Mechanical Engineering Series.* Marcel Dekker. New York. 177–205.

Lee, H. and Kim, H. (2003). CVT ratio control for improvement of fuel economy by considering power-train response lag. *KSME Int. J.* **17**, **11**, 1725–1731.

Mattson, P. (1994). An infinitely variable spilt-power transmission with a traction ball drive variator. *VDI Berichte*, **1170**, 137–152.

Mucino, V. H., Lu, Z., Smith, J. E., Kimcikiewicz, M. and Cowan, B. (2001). Design of continuously variable power split transmission systems for automotive applications. *Proc. Instn. Mech. Engrs.: Part D*, **215**, 469–478.

Norton, R. L. (2000). *Machine Design - An Integrated Approach.* 2nd edn. Prentice-Hall. New Jersey.

Pfiffner, R., Guzzella, L. and Onder, C. H. (2003). Fuel-optimal control of CVT powertrains. *Control Engineering Practice* **29**, **11**, 329–336.

Pichard, J. and Besson, B. (1981). Hydrostatic power splitting transmissions design and application example. *ASME J. Engineering for Power*, **103**, 168–173.

Russner, D. R. and Singh, Y. P. (2004). Design of input coupled split power transmissions, arrangements and their characteristics. *Trans. ASME*, **126**, 542–550.

Ryu, J. H., Kim, Y. K. and Park, N. G. (2002). A split power continuously variable transmissions (SPCVT) for bicycle use. *Proc. Small Engine and Transmission Conf.* JSAE 20024265, Kyoto, Japan.

Seong, S. H., Ryu, J. H., Lee, H. W. and Park, N. G. (2005). Conceptual design of inner-spherical continuously variable transmission for bicycle usage. *Int. J. Automotive Technology* **6**, **5**, 467–473.

Shoji, A. and Kawashima, G. (2002). The Development of the traction drive mechanism made of the plastic magnet. *Proc. Design Engineering Technical Conf. and Computers and Information in Engineering Conf.*, Illinois, USA.

Tanaka, H. and Eguchi, M. (1991). Speed ratio control of a half-toroidal traction drive CVT. *JSME Int. J. Ser. C*, **91-0375 B**, 203–211.

Tanaka, H. and Machida, H. (1996). Half-toroidal traction-drive continuously variable power transmission. *Engineering Tribology* **210**, **3**, 205–2.

Walker, J. (1994). Three new mechanical-hydrostatic power-split transmissions unveiled at IAA. *High Speed Diesels & Drives*, Chicago.